Analysis of circular and cylindrical array arrangements for mmwave 5G beamforming techniques

Analysis of circular and cylindrical array arrangements for mmWave 5G beamforming techniques

Daniel G. Riviello and Francesco Di Stasio
Department of Electronics and Telecommunications (DET)
Politecnico di Torino
Torino, Italy
Email: {daniel.riviello, francesco.distasio}@polito.it

***Abstract*—In this paper, we study the performance of a 5G base station working in the mmWave range equipped with a cylindrical array. Conventional and Capon beamforming techniques are taken into account. We consider both isotropic and directive antenna elements and we evaluate the trade-off between antennas per ring and number of rings with fixed number of total antennas. Results are provided in terms of average achievable per-user rate with different system configurations, such as of network loading. We show that in the presented scenario, where users are randomly deployed in a hexagonal plane, the best performance occurs when the cylindrical array degenerates in a circular array.**

***Index Terms*—Beamforming, circular array, cylndrical array, 5G, mmWave.**

I. Introduction

New technologies able to offer increased cellular capacities will be required due to the growing demand for higher data rates in mobile communications. A promising solution for 5G cellular systems is represented by the millimeter-wave (mmWave) frequency spectrum: hundreds of times more capacity than current 4G cellular networks are expected to be achieved [1]. Available bandwidths in the mmWave frequency spectrum considered for 5G are up to 200 times greater than all current cellular allocations [2], [3]. Thanks to the small wavelengths, implementation of massive MIMO techniques, array processing and beamforming (BF) will be possible. However, mmWave brings new challenging impairments which can increase the outage probability such as increased free space path loss attenuation due to rainfall and so far. The increased path loss will be compensated by the larger number of antennas, which also will allow better management of the inter-user interference, thanks to advanced BF techniques. New massive MIMO and BF algorithms that resort to advanced signal processing techniques have been proposed for 5G [5]–[7], but most of them implement these algorithms on Uniform Linear Arrays (ULAs) or Uniform Planar Arrays (UPAs).

In this paper, we evaluate the performance of a 5G cellular network operating in the mmWave range with a single base station (BS) equipped with an array of both isotropic and directive antennas capable of performing directional beamforming performing both conventional BF and Minimum Variance Distortionless Response (MVDR) [4] towards the users of interest. We also use some stochastic geometry concepts [9], [10], as single-antenna users are distributed according to a Binomial point process in $\mathcal{R}^2$. Moreover, we evaluate the trade-off between antennas per ring and number of rings with fixed number of total antennas N. The results are provided in terms of average per-user achievable rate with different system configuration, such as traffic loading or BF technique.

The paper is organized as follows: Sec. II describes the system model, Sec. III illustrates the mathematical framework for circular and cylindrical arrays, in Sec. IV, the beamforming techniques and examples of array radiation patterns are presented. The results are shown and discussed in Sec. V and finally Sec. VI draws the conclusions.

II. System Model

Let us consider an hexagonal cell of circumradius R in which K single-antenna users communicate with a Base Station (BS) located at the center of the hexagon, with height h from the ground equipped with an array of N antennas.

A. Spatial point process

Users are modeled as a spatial Binomial point process (BPP) with $h = 0$. If we consider a bounded region $\mathcal{A}$ of the plane, with $|\mathcal{A}| = \pi R^2$ the area of the circumcircle, and M the number of nodes existing in the region $\mathcal{A}$, then the number of nodes in the bounded area $\mathcal{B} \subset \mathcal{A}$, with $|\mathcal{B}| = \frac{3\sqrt{3}}{2}R^2$ the area of the hexagon, is a random variable denoted by $\Phi(\mathcal{B})$. The probability of K nodes existing in $\mathcal{A}$ is given by:

$$\Pr[\Phi(\mathcal{B}) = K] = \binom{M}{K} \left(\frac{|\mathcal{B}|}{|\mathcal{A}|}\right)^K \left(1 - \frac{|\mathcal{B}|}{|\mathcal{A}|}\right)^{M-K} \quad (1)$$

i.e., K is a Binomial random variable $Bin(n, p)$ with parameters $n = M$ and probability $p = \frac{|\mathcal{B}|}{|\mathcal{A}|} = \frac{3\sqrt{3}}{2\pi}$:

$$K \sim Bin\left(M, \frac{3\sqrt{3}}{2\pi}\right) \quad (2)$$

By definition of a BPP, the nodes are conditionally independent and the locations uniformly distributed in the hexagon.

B. Baseband model

We focus on the uplink communication between K users and the BS . Let $\mathbf{x} = [x_1, x_2, \ldots, x_K]^T$ be the vector of symbols transmitted by the K users in a given time slot and carrier, each with power $E[|x_i|^2] = P_i$. The baseband equivalent signal vector received by the N antennas at the BS is hence given by $\mathbf{y} = \mathbf{H}\mathbf{x} + \mathbf{n}$, where $\mathbf{H} = [\mathbf{h}_1, \mathbf{h}_2, \ldots, \mathbf{h}_K]$ is the $N \times K$ wireless channel matrix. Each vector $\mathbf{h}_i \in \mathcal{C}^{N\times 1}$ represents the propagation channel vector from user i to the BS and $\mathbf{n} \sim \mathcal{CN}(0, \sigma_n^2\mathbf{I})$ is the spatially uncorrelated Gaussian noise vector. A simplified channel model, nevertheless suitable for mmWave systems, is taken into account. The propagation in mmWave bands is mostly Line of Sight (LOS) with a diffusive component [2], The channel vector for the i-th user is $\mathbf{h}_i = \sqrt{\gamma_i}\,\beta_i\,\mathbf{a}(\theta_i, \phi_i)$. where the path loss γ_i is equal to $\gamma_i = \left(\frac{\lambda}{4\,\pi\,d_i}\right)^2$. Moreover, d_i is the distance of the i-th user from the BS and β_i is the Rician fading gain affecting the link between the i-th user and the BS with Rician factor R_{F}. In addition, $\mathbf{a}(\theta_i, \phi_i)$ represents the steering vector (SV) or array response for the Direction of Arrival (DoA) of the i-th user with elevation angle θ_i and azimuth ϕ_i. In order to guarantee fairness among users, we adopt a simple power control mechanism and we assume that each user is assigned a transmit power P_i that is a fraction of the maximum transmit power P_{max} and compensates for the path loss $P_i = P_{max}\,d_i^2/(h^2 + R^2)$.

Perfect channel state information (CSI) at the BS is assumed. Moreover, we assume that the BS is serving K users in the same resource (same time slot and bandwidth), and at least K RF chains or parallel beamformers ($K < N$). The BS resorts only to Space Division Multiple Access (SDMA) through BF. The BS processes the K signals through the combining matrix $\mathbf{B} = [\mathbf{b}_1^H|\mathbf{b}_2^H|\ldots|\mathbf{b}_K^H] \in \mathcal{C}^{K\times N}$, where $\mathbf{b}_i$ is the $N \times 1$ beamformer or spatial filter designed for the i-th signal of interest with DoA (θ_i, ϕ_i), so that it attenuates all the other DoAs. The final estimated signal ensemble is given by $\hat{\mathbf{x}} = \mathbf{B}\mathbf{y}$ with decision variable for the i-th user $\hat{x}_i = \mathbf{b}_i^h\mathbf{y}$. We can finally express the instantaneous Signal-to-Noise-plus-Interference ratio at decision variable $\hat{x}_i$ as:

$$SINR_i = \frac{P_i\,|\mathbf{b}_i^H\mathbf{h}_i|^2}{\sigma_n^2|\mathbf{b}_i|^2 + \sum\limits_{\substack{k=1\\k\neq i}}^{K} P_k|\mathbf{b}_i^H\mathbf{h}_k|^2}. \tag{3}$$

The achievable rate for each user i is defined as $C_i = \log_2(1 + SINR_i)$, results in this paper will be presented with the metric of the average per-user achievable rate $C = \mathrm{E}[C_i]$ where expectation $\mathrm{E}[\cdot]$ is with respect to fading and users' positions.

III. Array processing

In this Section, we will describe how to express the array response (SV) $\mathbf{a}(\theta_i, \phi_i)$ for a generic i-th user when the BS is equipped with a Uniform Circular Array (UCA) or Uniform Cylindrical Array (UCylA) with both isotropic and directive antenna elements. We denote with $N = N_c \cdot N_z$ the total number of available antennas at the BS, where N_c is the number of antennas in each ring, while N_z denotes the number of rings, or equivalently the number of antennas along the z-axis. Perfect calibration of the arrays is assumed with no mutual coupling among the antenna elements.

A. Uniform Circular Array

When the BS is equipped with a single ring of N_c isotropic antennas elements, i.e., a Uniform Circular Array (UCA), we first define the radius of the array $r = \lambda\,N_c/4\pi$ which guarantees $\lambda/2$ spacing on the circular arc between elements. We can then write the $N_c \times 1$ array response or SV $\mathbf{a}_{\text{UCA}}(\theta_i, \phi_i)$ for the DOA of the i-th user as:

$$\mathbf{a}_{\text{UCA}}(\theta_i, \phi_i) = \begin{bmatrix} e^{j\frac{N_c}{2}\sin\theta_i\cos\phi_i} \\ e^{j\frac{N_c}{2}\sin\theta_i\cos\left(\phi_i - \frac{2\pi}{N_c}\right)} \\ \vdots \\ e^{j\frac{N_c}{2}\sin\theta_i\cos\left(\phi_i - 2\pi\frac{N_c-1}{N_c}\right)} \end{bmatrix} \tag{4}$$

B. Uniform Cylindrical Array

Now we can define a SV for a Uniform Cylindrical Array (UCylA). The array is made of N_z horizontal ring sub-arrays, spaced vertically at half wavelength, with N_c elements per ring. First, we define the $N_z \times 1$ SV of the Uniform Linear Array (ULA) lying on the z-axis as:

$$\mathbf{a}_{\text{ULA}}(\theta_i) = \left[e^{-j\pi\frac{N_z-1}{2}\cos\theta_i}, \ldots, e^{j\pi\frac{N_z-1}{2}\cos\theta_i}\right]^T \tag{5}$$

where the phase reference point is the center of the cylinder. The global $N \times 1$ SV of the UCylA is the Kronecker product of the 2 SVs, i.e. $\mathbf{a}_{\text{UCylA}}(\theta_i, \phi_i) = \mathbf{a}_{\text{UCA}}(\theta_i, \phi_i) \otimes \mathbf{a}_{\text{ULA}}(\theta_i, \phi_i)$.

C. Directive antenna elements

We now redefine the expressions of the SVs when the array is equipped with directive antenna elements. Directivity is assumed only for the azimuthal plane, while the antennas are isotropic w.r.t. the elevation angle, therefore we define the directivity function of the single antenna as:

$$D(\phi_i) = \begin{cases} u\cos(\phi_i - \delta) & \text{for } -90^\circ + \delta < \phi_i < 90^\circ + \delta \\ 0 & \text{otherwise} \end{cases} \tag{6}$$

where u is a scaling factor and δ the azimuthal direction to which the antenna element is pointed.

1) Circular array with directive elements: Let us denote with $\mathbf{d}(\phi_i)$ the $N_c \times 1$ vector, which contains the values of the directivity function $D(\phi_i)$ associated with each element of the UCA. The generic directivity element can be espressed as $d_n(\phi_i) = u\cos\left(\phi_i - 2\pi\frac{n}{N_c}\right)$, where $n = 0, 1, \ldots, N_c - 1$. It is easy to verify that, due to shadowing, half of the elements will be equal to zero in accordance with (6). The resulting $N_c \times 1$ SV of the UCA with directive antenna elements is equal to $\mathbf{a}_{\text{UCA}}^{(d)}(\theta_i, \phi_i) = \mathbf{d}(\phi_i) \odot \mathbf{a}_{\text{UCA}}(\theta_i, \phi_i)$, where $\odot$ denotes the Hadamard (entrywise) product.

2) Cylindrical array with directive elements: The $N \times 1$ SV for a UCylA with directive antenna elements becomes $\mathbf{a}_{\text{UCylA}}^{(d)}(\theta_i, \phi_i) = \mathbf{a}_{\text{UCA}}^{(d)}(\theta_i, \phi_i) \otimes \mathbf{a}_{\text{ULA}}(\theta_i, \phi_i)$.

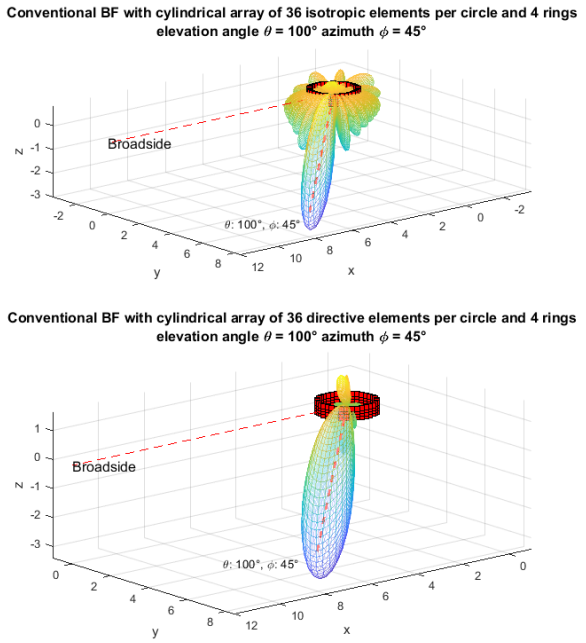

Fig. 1: Pattern with conventional BF for a 36×4 UCylA for DoA $(100°, 45°)$ with isotropic and directive antenna elements.

IV. Beamforming methods

We focus now on the design of the beamformer $\mathbf{b}_i$ design whose tasks are to correctly estimate the i-th signal of interest and attenuate interferers. Two different algorithms are taken into account for analysis: Conventional BF and Minimum Variance Distortionless Response (MVDR) BF or Capon BF.

A. Conventional beamforming

With this approach, also known as beam steering, the BS produces a phase shift to compensate for the delay of the DOA (θ_i, ϕ_i) for the i-th user, which is given by $\mathbf{b}_i = \mathbf{a}(\theta_i, \phi_i)$.

B. MVDR beamforming

For MVDR BF, we first introduce the global spatial covariance matrix of noise plus interference for:

$$\mathbf{R} = \sigma_n^2 \mathbf{I} + \sum_{k=1}^{K} P_k \, \gamma_k \, \mathbf{a}(\theta_k, \phi_k) \, \mathbf{a}^H(\theta_k, \phi_k) \tag{7}$$

Beamforming is then a constrained optimization problem that maximizes the power towards the i-th user of interest and minimizes the overall interference arising from other DoAs [4]:

$$\mathbf{b}_i = \frac{\mathbf{R}^{-1} \, \mathbf{a}(\theta_i, \phi_i)}{\mathbf{a}^H(\theta_i, \phi_i) \, \mathbf{R}^{-1} \, \mathbf{a}(\theta_i, \phi_i)} \tag{8}$$

Notice that the denominator $\mathbf{a}^H(\theta_i, \phi_i) \, \mathbf{R}^{-1} \, \mathbf{a}(\theta_i, \phi_i)$ in (8) is a normalization factor and ensures unitary gain at the DoA of interest.

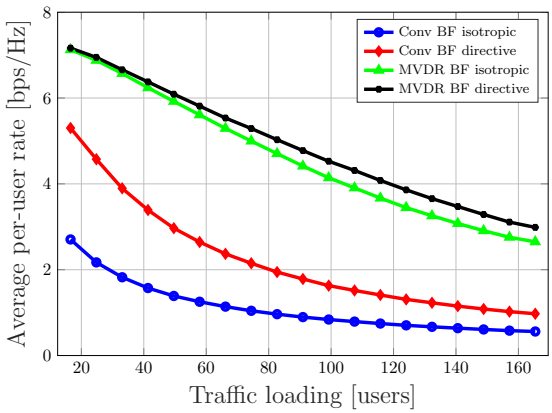

Fig. 2: Average per-user rate as a function of the network load (average number of users in $\mathcal{B}$). Comparison for a UCylA with isotropic and directive antennas, implementing conventional and MVDR BF. N_c=90, N_z=4

C. Patterns with isotropic and directive antennas

The array gain function, when the beamformer is designed for the DoA (θ_i, ϕ_i) of the i-th user, can be defined for any DoA (θ, ϕ) as $\mathbf{G}(\theta, \phi \,|\, \theta_i, \phi_i) = |\mathbf{b}_i \, \mathbf{a}(\theta, \phi)|^2$, the array radiation pattern or array factor AF is equal to $AF(\theta, \phi \,|\, \theta_i, \phi_i) = \sqrt{\mathbf{G}(\theta, \phi \,|\, \theta_i, \phi_i)}$ and in the case conventional BF it has very well known expressions for linear, planar [11] and circular arrays [8].

Fig. 1 shows the radiation pattern with conventional BF for a DoA $(100°, 45°)$ of a UCylA with 4 rings along z and 36 isotropic (directive) elements per ring on the top (bottom). By focusing on the azimuthal plane, the beam remains constant for the UCA regardless of ϕ and the main lobe is wider with directive antennas w.r.t. isotropic ones, since half of the elements actually contribute to the pattern, but it is worth noticing that for the same reason, sidelobes are almost suppressed, bringing improvements in terms of interference rejection capability.

V. Results

We compare now the performance of a BS equipped with a UCylA with both isotropic and directive antennas in terms of average-per-user rate with both conventional and MVDR BF. We suppose that the BS is working at $f_c = 25$ GHz with a total bandwidth $B = 100$ MHz and a maximum transmitted power of $P_{max} = 20$ dBm, and it is equipped with a total number of antennas $N = 360$. Moreover, the BS is fixed at an height of 15 m at the center of a hexagonal cell of area $|\mathcal{B}| = 0.1039$ km^2, the circumrcircle of the cell has a radius $R = 200$ m with an area $|\mathcal{A}| = 0.1258$ km^2. We assume that the network load (number of users M in $\mathcal{A}$) is equal to 60, the noise figure F has been fixed to 7 dB and the Rician factor $R_{\text{F}} = 10$. Finally, we consider the directivity function given by $D(\phi_i) = 2\cos(\phi_i - \delta)$.

Fig. 2 shows the average per-user rate C as a function of the network load or average number of users in the hexagonal cell $\mathcal{B}$, computed as the mean of a Binomial random variable

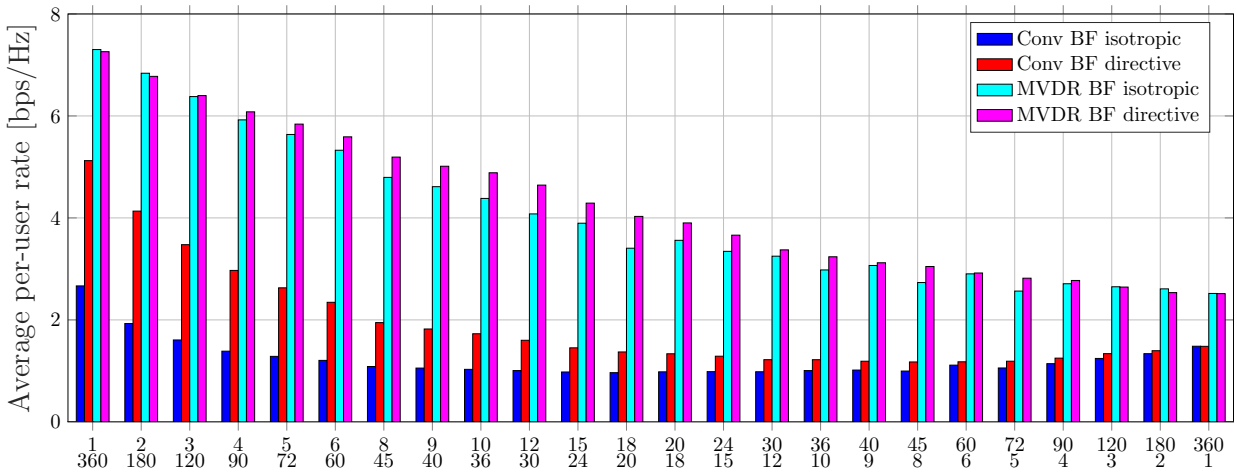

Fig. 3: Average per-user rate in UCylA for different number of rings N_c and antennas along z-axis N_z with both isotropic and directive elements implementing conventional and MVDR BF with $N = N_c \cdot N_z = 360$. For $N_c = 1$, $N_z = 360$, antennas are only isotropic. $M = 60$ users.

$\mathrm{E}(K) = M\frac{3\sqrt{3}}{2\pi}$, with M ranging from 20 to 200 users in the circumcircle, the UCylA has $N = 360$ total antennas, with $N_c = 90$ rings and $N_z = 4$ elements per ring. It clearly confirms how MVDR is able to outperform conventional BF thanks to its improved interference rejection capability, but it also shows that directive elements provide a significant rate improvement w.r.t. isotropic elements for conventional BF. The gap is more than 2 bps/Hz for low network loads and it reduces as the network load increases; for the MVDR BF case, the overall performance decreases more slowly and the gap between directive and isotropic antennas is much smaller, but it slightly increases as the number of users increase.

Now, we investigate on the distribution of antenna elements along the vertical axis and the azimuthal plane by keeping constant the total number of antennas N. Fig. 3 shows a bar plot with the average per-user rate for different configurations of N_c antennas per ring and N_z rings or antennas along the z-axis, with fixed $N = 360$, both isotropic and directive elements with conventional and MVDR BF, $M = 60$ users in the area $\mathcal{A}$. The key result here is that, within the presented scenario in which all users lie on a plane at the ground level ($h = 0$), for all configurations the best performance occurs when all antennas are arranged in a single UCA or ring: this suggests that producing narrower beams along ϕ offers better interference rejection capability than along θ. It can also be noted that in the configuration $N_z = 360$, $N_c = 1$, the array degenerates into a ULA along z (only isotropic elements are used for this specific configuration). Finally, for conventional BF, there is a slight trend inversion in the performance as the UCylA almost degenerates into a ULA.

VI. Conclusions

The performance of a 5G Base Station equipped with a Uniform Cylindrical Array and working in the mmWave region with both isotropic and directive antenna elements has been evaluated considering Conventional and Capon beamforming. The results, shown in the form of achievable average per-user rate with different configurations, have confirmed the improved interference rejection capability of the MVDR technique. The trade-off between antennas per ring and number of rings with fixed number of total antennas has been carried out and it has shown that in the presented scenario, with randomly deployed users in a hexagonal plane, the best performance occurs when the cylindrical array degenerates in a circular array.

References

[1] W. Roh, J. Seol, J. Park, B. Lee, J. Lee, Y. Kim, J. Cho, K. Cheun and F. Aryanfar, "Millimeter-wave beamforming as an enabling technology for 5G cellular communications: theoretical feasibility and prototype results," *IEEE Communications Mag.*, pp. 106-113, Feb. 2014.

[2] M. R. Akdeniz, Y. Liu, M. K. Samimi, S. Sun, S. Rangan, T. S. Rappaport and E. Erkip, "Millimeter Wave Channel Modeling and Cellular Capacity Evaluation", *IEEE Journal on Selected Areas in Communications*, vol. 32, no. 6, pp. 1164-1179, June 2014.

[3] T. S. Rappaport, W. Roh, and K. Cheun, "Mobiles millimeter-wave makeover," *IEEE Spectrum*, pp. 35-56, Sep. 2014.

[4] J. Capon, "High-Resolution Frequency-Wavenumber Spectrum Analysis," *Proceedings of the IEEE*, vol. 57, no. 8, pp. 1408-1418, Aug. 1969.

[5] R. W. Heath, N. Gonzlez-Prelcic, S. Rangan, W. Roh and A. M. Sayeed, "An Overview of Signal Processing Techniques for Millimeter Wave MIMO Systems," in *IEEE Journal of Selected Topics in Signal Processing*, vol. 10, no. 3, pp. 436-453, Apr. 2016.

[6] O. E. Ayach, S. Rajagopal, S. Abu-Surra, Z. Pi and R. W. Heath, "Spatially Sparse Precoding in Millimeter Wave MIMO Systems," in *IEEE Transactions on Wireless Communications*, vol. 13, no. 3, pp. 1499-1513, Mar. 2014.

[7] A. Alkhateeb, J. Mo, N. Gonzalez-Prelcic and R. W. Heath, "MIMO Precoding and Combining Solutions for Millimeter-Wave Systems," in *IEEE Communications Magazine*, vol. 52, no. 12, pp. 122-131, Dec. 2014.

[8] L. Josefsson and P. Persson, *Conformal Array Antenna Theory and Design*, John Wiley, Hoboken, NJ, Chapter 6, 2006.

[9] M. Haenggi, "On distances in uniformly random networks", *IEEE Transactions on Information Theory*, vol. 51, no. 10, pp. 3584-3586, Oct. 2005.

[10] S. Srinivasa and M. Haenggi, "Distance Distributions in Finite Uniformly Random Networks: Theory and Applications", *IEEE Transactions on Vehicular Technology*, vol. 59, no. 2, pp. 940-949, Feb. 2010.

[11] Balanis, Constantine A, *Antenna theory: analysis and design*, Wiley-Interscience, 2005.